Optics Communications 547 (2023) 129852

Contents lists available at ScienceDirect

Optics Communications

journal homepage: www.elsevier.com/locate/optcom

Transient dynamics in mode-locked all-PM Er-doped fiber laser with NALM

D. Stoliarov [a,*], I. Kudelin [b,c], A. Koviarov [a], E. Rafailov [a]

[a] Aston Institute of Photonic Technologies, Aston University, Birmingham, B4 7ET, UK
[b] Time and Frequency Division, National Institute of Standards and Technology, Boulder, CO, 80305, USA
[c] Department of Physics, University of Colorado Boulder, Boulder, CO, 80309, USA

ARTICLE INFO

Keywords:
Polarization maintaining fiber
Q-switching
Mode locking
Nonlinear amplifying loop mirror
Time-stretch dispersive fourier transform
Soliton molecules
Bound state

ABSTRACT

In this study, we utilized the Time-Stretch Dispersive Fourier Transform (TS-DFT) method to explore rapid transient states in both time and frequency domains of an all-polarization-maintaining dispersion-managed figure-eight mode-locked laser with Nonlinear Amplifying Loop Mirror (NALM). We detail the different stages of build-up dynamics at varying pump powers, encompassing the Q-switching (QS) stage, transient single pulse formation, pulsation beating patterns, bound states, and the final transition to a single pulse state. Our findings reveal that the mode-locked bound state regime emerges from a single pulse stage following QS, different from previously reported directly resulting from QS pulses or relaxation oscillations. In a novel contribution to the field, we have experimentally demonstrated the transient single pulse stage of build-up dynamics and compared it with the fundamental mode-locked single pulse.

1. Introduction

Ultrafast fiber lasers, specifically mode-locked fiber lasers, have become irreplaceable instruments in various scientific and technological fields due to their ability to generate ultrashort pulses with high peak power with high stability [1,2]. These lasers have significantly impacted areas such as telecommunications, spectroscopy, and material processing [2,3]. The advent of all-polarization maintaining (all-PM) 8 and 9-figure mode-locked fiber lasers has further broadened these systems' capabilities. All-PM schemes are distinguished by their robustness, ease of use, and high stability performance, making them also highly advantageous in out-of-lab applications [4,5]. In comparison to other mode-locking mechanisms such as Semiconductor Saturable Absorber Mirrors (SESAMs) [6], Carbon nanotubes (CNT) [7] and Nonlinear polarization rotation (NPR) [8], employing Nonlinear Amplifying Loop Mirror (NALM) or Nonlinear-Optical Loop Mirror (NOLM) as a mode-locking device reduces the complexity of operation and maintenance. These advantages are key reasons why all-PM fiber lasers, based on NALM or NOLM, have found extensive use in contemporary commercial devices [9,10].

The study of nonlinear dynamics in mode-locked fiber lasers has gained prominence in recent years, aiming to improve performance and broaden application scope. A comprehensive understanding of nonlinear phenomena occurring in ultrafast lasers is vital for optimizing cavity design and functionality soliton formation and its evolution [11]. Recently, The time-stretch dispersive Fourier transform (TS-DFT) technique has notably advanced the study of these nonlinear dynamics [12], enabling researchers to uncover the transient and non-stationary properties of dissipative optical systems, which are 'invisible' for traditional diagnostic tools such as Optical Spectrum Anylzers (OSA), autocorrelators, frequency-resolved optical gating and monochromators, gaining a more thorough understanding of complex ultrafast phenomena [13]. These phenomena include soliton build-up dynamics [11,14], soliton explosions [13,15], soliton molecules [16,17], soliton distillation [18], and various pulsating soliton [19–22].

Wang etc. Presented an intermediate stage between continuous wave (CW) emission and noise-like pulses (NLPs) in an Er-doped partially mode-locked fiber laser employing nonlinear polarization rotation, where soliton bunches sporadically emerge from a quasi-CW background within the Q-switched-like envelope [23].

By using the DFT technique the complex build-up dynamics inside of laser modelocked-cavity could be successfully observed. Real-time access to multipulse interactions in a femtosecond laser oscillator facilitates the tracking of stable soliton molecule formation and reveals swift internal motions across a variety of bound states [24]. It was demonstrated that two soliton-pair molecules can bind subsequently to form a stable molecular complex and highlight the important differences between the intra-molecular and inter-molecular bonds [25].

* Corresponding author.
E-mail address: d.stoliarov@aston.ac.uk (D. Stoliarov).

https://doi.org/10.1016/j.optcom.2023.129852
Received 15 June 2023; Received in revised form 13 July 2023; Accepted 20 August 2023
Available online 23 August 2023

Despite significant strides, made in characterizing stable states, a substantial knowledge gap remains in understanding the buildup dynamics in all-PM critically influence laser overall operation and potential applications.

In all-PM fiber lasers, the transition from the unstable Q-switched pulses to the stable mode-locked regime involves complex dynamics, including the emergence and decay of multiple pulses. These pulses exhibit a wide range of dynamics, including the formation of multi-pulse states or soliton molecules [26,27]. In 2019, X. Liu and colleagues unveiled a novel soliton formation process in ultrafast lasers, involving four stages: initial spontaneous noise, Q-switching (QS), beating dynamics, and mode-locking (ML) [11]. This process featured multiple subnanosecond pulses co-existing in the laser cavity during QS, with one dominant pulse evolving into a soliton during ML. A theoretical model was proposed to simulate the spectro-temporal beating dynamics (crucial for QS-ML transition) and the Kelly sidebands of the formed solitons. The numerical results, in line with experimental observations, illustrated that beating dynamics were triggered by the interference between a dominant pulse and multiple subordinate pulses with variable temporal delays.

The specific pulse evolution can vary between measurements, but the general dynamics involve the emergence of multiple pulses from noise, followed by their subsequent decay. This behaviour is characteristic of the transient regime and provides valuable insights into the internal evolution of solitons in a mode-locked fiber laser. Moreover, similar build-up dynamics have been observed in various ultrafast lasers, including Ti:Sapphire [28], NPR [29], and even bidirecional mode-locked lasers [30,31].

Achieving self-starting passive mode-locking without an amplitude modulator has proven challenging. One of the most widely used techniques for Erbium (Er) doped all-PM fiber lasers is over pump method. Numerous regimes were initially observed in these lasers, ranging from noise-like pulses to soliton bunching and soliton molecules. The transition to a stable single-pulse regime was achieved by reducing the pump power [32]. One of the most intricate dynamics is observed in dispersion-managed all-PM fiber lasers with NALM [33]. These lasers implement dispersion management using fiber spans of alternating dispersion, leading to the periodic stretching and recompression of pulses in every resonator round trip. Theoretical and experimental research has shown that the net dispersion of a NALM can greatly influence the build-up time of mode-locking [34–36]. In certain instances, particularly with dispersion-imbalanced (DI) NALM in a figure-eight scheme, the build-up time could extend to as long as 8 min [32]. The transition dynamics from QS to a stable ML state is of particular interest, as this process may necessitate more than 10 thousand pulse roundtrips. Therefore, all-PM Er fiber lasers employing a DI-NALM could provide an ideal testbed system for studying this long-duration transition dynamics.

In this paper, we present, for the first time to our knowledge, direct observation, utilizing the TS-DFT, of the lengthy transition dynamics composed of alternating transient bound states and beating dynamics during soliton formation and its evolution. This is analyzed in the transition phase from QS to ML in all-PM figure-eight fiber laser. The transient stages are analyzed in both the time and frequency domains. By applying the Fast Fourier Transformation (FFT), we elucidate the evolution dynamics of pulse separation, represented as field autocorrelation of each single-shot spectrum [29,31], when solitons are generated via Q-switched and single transient pulse. This stands in contrast to solitons originating from relaxation oscillations (or quasi-continuous-wave oscillations) [28] or beating dynamics [37]. In the final phase of our study, we leveraged the capabilities of the TS-DFT method to measure rapid transient states within the laser cavity. This allowed us to compare the single transient pulse observed at the onset of the mode-locked build-up dynamics with the fundamental single pulse regime, achieved through a reducing the pump power of the laser. The observed transition from a dual-pulse to a single pulse in our study occurred in fewer than 10 roundtrips, a significantly more rapid dynamic compared to other studies [38]. This fast transition broadens the potential applications of all-PM lasers that are based on NALM loops. The archived in this work results offer additional insights into the evolution and characteristics of different pulse regimes in all-PM fiber lasers, contributing to a more profound understanding of its intricate dynamics and potential for further optimization.

2. Experimental setup and principle

The experimental configuration of the dispersion-managed, figure-of-8 oscillator is delineated in Fig. 1. The cavity, assembled from single-mode, polarization-maintaining fibers and components (PANDA style), is composed of two parts.

(i) The unidirectional resonator (UR) loop incorporates a 0.6-m segment of PM Erbium-Doped Fiber (EDF) ER80-4/125-HD-PM (nLight), excited by a 980 nm laser diode via a polarization-maintaining 980/1550 Wavelength Division Multiplexing (WDM) coupler. An optical isolator (ISO) within the main loop ensures unidirectional propagation of the intra-cavity pulse. A substantial length of Dispersion Compensation Fiber (DCF) PM2000D (Coherent) is employed to counteract the anomalous dispersion inherent to the SMF fiber (PM1550-XP) at 1550 nm. The configuration of the Unidirectional Ring (UR) loop incorporates a narrow bandpass filter (BPF) centered at 1550 nm with a full width at half-maximum (FWHM) bandwidth of 2 nm. This filter plays a crucial role in achieving stable mode-locking operation, a process that is facilitated by the filtering effects within the cavity. These effects ensure compliance with the cavity boundary conditions. While the filtering action can be achieved through the use of a bandpass filter or a saturable absorber, it can also inherently emerge from the finite gain bandwidth of the active fiber. In the mode-locked regime, the spectrum is notably broader than the 2 nm bandwidth of the bandpass filter. This observation underscores the occurrence of significant pulse evolution and nonlinear spectral broadening within the laser during each round trip. A 90/10 coupler (Output OC) extracts 10% of the cavity power, serving as the laser output.

(ii) The dispersion-imbalanced Nonlinear Amplifying Loop Mirror (DI-NALM), a critical component of the system, incorporates a 0.3-m segment of the same PM EDF used in the main loop. Note that the EDF has a normal group-velocity-dispersion (GVD) of 20 ps^2/km in contrast to the passive PM1550-XP fibers with a negative GVD of −22 ps^2/km at 1550 nm. This NALM loop is excited by 980 nm laser diode through the WDM coupler. In addition to the PM-EDF, the NALM loop incorporates a significant length of polarization-maintaining DCF with GVD around 64 ps^2/km at 1550 nm. This DCF serves a dual purpose: it compensates for dispersion and simultaneously augments the asymmetry of the loop. The NALM loop is linked with the main loop through a 60/

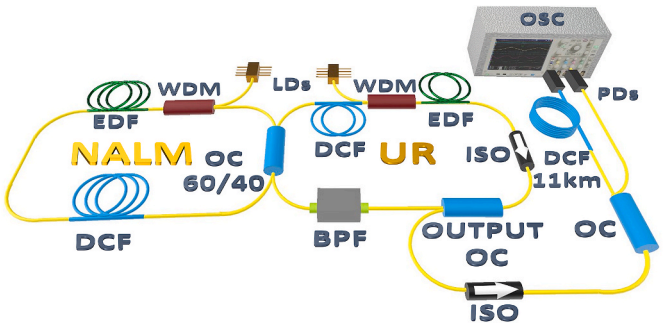

Fig. 1. Schematic diagram of the experimental setup for the figure-of-8 all-PM fiber mode-locked laser.

40 coupler, thereby establishing a robust and efficient connection between the two loops. A 60/40 optical coupler (OC 60/40) is utilized to induce a minor loop asymmetry and a nonlinear phase shift between the clockwise and counterclockwise propagating pulses. The two pieces of DCF fibre in both loops compensate for the total dispersion of the cavity, thereby approximating the net cavity dispersion to 0.07 ps^2. Both WDMs and ISO house a polarizer to block the fast axis, ensuring the entire cavity maintains polarization, thereby producing a linearly polarized output pulse. The total length of the laser was 19.5 m, so the pulse repetition rate was measured as 10.6 MHz.

By simply adjusting the pump power level in both loops, we gain two degrees of freedom to fine-tune the output characteristics of the mode-locked oscillator. We showcase a mode-locked PM figure-eight Er fiber laser with a dispersion-imbalanced NALM. An over-pumping method was employed to trigger nonlinear evolution, with the DI-NALM contributing to self-started mode-locking. Once mode-locking has started, the pump power was then reduced to a level where stable, high-quality single pulses can be generated. The NALM was constructed based on the asymmetric positioning of the anomalous dispersion, Erbium-doped, and DCF fibers. This configuration resulted in asymmetric pulse amplification and broadening, which was instrumental in initiating self-started mode-locking.

To record the DFT traces we, at first, set the pump power in both loops for initial generation in a multi-pulse regime. Then, the switching of the power of the pump lasers initiates Q-switched pulse generation, which triggers the oscilloscope to record the trace. To convert the temporal profile into spectra, we used 11 km of normal dispersion compensating fibre (DCF 11 km) with total dispersion of −1200 ps/nm. The stretched spectral profile was subsequently detected via 50 GHz photodiodes (PDs) Finisar XPDV2320R in tandem with a high-speed 33 GHz bandwidth oscilloscope (OSC) DSOX93204A Agilent. The resolution of the TS-DFT, limited by the bandwidth of the used electronic, was 0.025 nm. Accordingly, the first-order autocorrelation, obtained by FFT of the TS-DFT trace, has a maximum time delay of 360 ps with a fs-level resolution by zero-padding the TS-DFT traces. Thus, the single-shot spectral interferograms were directly recorded, providing real-time insights into the dynamics within the complex ultrafast soliton structures.

3. Results and discussion

In contradistinction to the modelocked build-up dynamics evident in fiber ring lasers with CNT absorbers as delineated in the studies by Liu [11,37], our empirical investigations have revealed a divergent behaviour and ancillary transient phases. It is apparent that this discrepancy transpires due to disparate modelocked mechanisms operating within the laser cavity. Furthermore, the net cavity dispersion in our experimental configuration was effectively manipulated to the normal range through the integration of Dispersion Compensating Fiber (DCF) into both loops of the cavity.

Our research endeavoured to concentrate on the meticulous exploration of the formation dynamics of beating and extended-bound state solitons during the intermediary phase transitioning from Q-switching (QS) to mode-locking (ML) in all-polarization maintaining (PM) fiber lasers with dispersion-imbalanced Nonlinear Amplifying Loop Mirror. Analogously to the mode-locked ring lasers equipped with CNT film and modulated pumps as expounded in the investigation by Xueming Liu - wherein they identified four build-up stages - the build-up dynamics of our overpumped all-PM ML laser could be delineated into six discernible stages: Relaxation Oscillations (RO), Q-switching (QS), a Single Pulse stage, Beating Dynamics (BD), a transient Bound State (BS), and ultimately, a Stable Bound State Mode-locking (BS ML).

As previously noted, the placement of the DCF in the NALM scheme could play a pivotal role in the buildup time, particularly in the BD and transient BS stages. In our laser scheme, the first BS is completed in less than a hundred roundtrips. However, the transient BS stage is the longest transient stage, during which the periodically occurring beating dynamics stages were observed. The pre-stable mode consists of a transient bound state, and BD stages persist for more than 8 thousand roundtrips before the stable bound state is achieved.

In the initial step, we employed over-pumping using two 980 nm Laser Diodes (LDs) to ensure ample pump power for achieving self-started mode-locking. Upon activating the LDs, the powerful QS state typically commenced after RO. RO stage is typically characteristic of the transient behaviour of lasers, as demonstrated by Liu et al. who experimentally established that multiple subnanosecond pulses appear during this stage, with only one dominant pulse evolving into the stationary mode-locked soliton. As such, only the most robust pulse endures, while the others dissipate [37]. In our experiment, we bypassed the consideration of the RO stage and instead concentrated on the transient stages subsequent to QS. The roundtrip count in our experiment commenced from the midpoint of the final RO stage. We underscore that no adjustments were made to the other parameters of this laser; the pump power was the sole modified variable. As mentioned earlier, the build-up process in this type of laser could span minutes. In our instance, it took a matter of a few seconds to attain the QS pulse. From the experimental results shown in Fig. 2 (b), it is evident that the transition phase between QS and the stable bound state involves periodically alternating between multiple beatings and unstable bound-state mode-locking stages. This transition phase spans about 7400 round trips, equivalent to roughly 0.7 ms. This duration was adequate for conducting DFT measurements of transient bound states and the production of stable soliton molecules.

Using the TS DFT technique, we successfully captured the evolution of the laser on a shot-by-shot basis, as illustrated in Fig. 3. Fig. 3 (a) presents our real-time experimental observations via a series of interferograms, comprehensively tracing the entire formation process of a stable mode-locked (ML) bound state. Fig. 3 (b) provides close-up views of the four regions highlighted in Fig. 3(a). Fig. 3 illustrates that following the Q-switching (QS) stage, the soliton evolution in the mode-locked laser transitions through various stages, including a transient single pulse, beating dynamics, and a transient bound state. The transient single pulse emerged for a duration of less than 100 round trips following the QS stage. Interestingly, no beating behaviour was observed between the QS stage and the transient single pulse stage, as is apparent from the magnified view in Fig. 3 (b). However, beating dynamics became apparent during the formation of the transient bound state.

During the first beating dynamic process, a single soliton splits into four. Subsequently, the transient bound state emerges, characterized by intense interaction among the newly formed solitons. To elucidate the formation and development of the bound state, we have revisualized the data from Fig. 3 (a) in Fig. 4. The Fourier transform of each individual shot spectrum equates to the field autocorrelation of the instantaneous bound-state solitons, thereby tracking the separation between the solitons, as depicted in Fig. 4 (a). The real-time data reveal the intricate temporal evolution, for instance, the emergence of four solitons from a single soliton near the 600th round-trip. The internal dynamics of the soliton molecule are exceptionally complex, exhibiting multipulse interactions, which can be visualized through the temporal separations between the solitons, as demonstrated in Fig. 4. Fig. 4(b–d) depict the intricate evolution ofpulse autocorrelation trace dynamics in three dimensions, with multiple coexisting pulses. This evolution showcases the presence of several soliton molecules with distinct structures that restructure following the beating stages. In our all-PM fiber scheme, we utilized an over-pumping technique to instigate the formation of bound states. Given the high degree of pumping applied to the cavity, the excitation of multiple solitons is an expected outcome. These solitons subsequently undergo a complex set of dynamics to attain a stable operation in a multi-soliton regime. In order for the bound states to transition into a stable single-pulse mode-locked regime, we

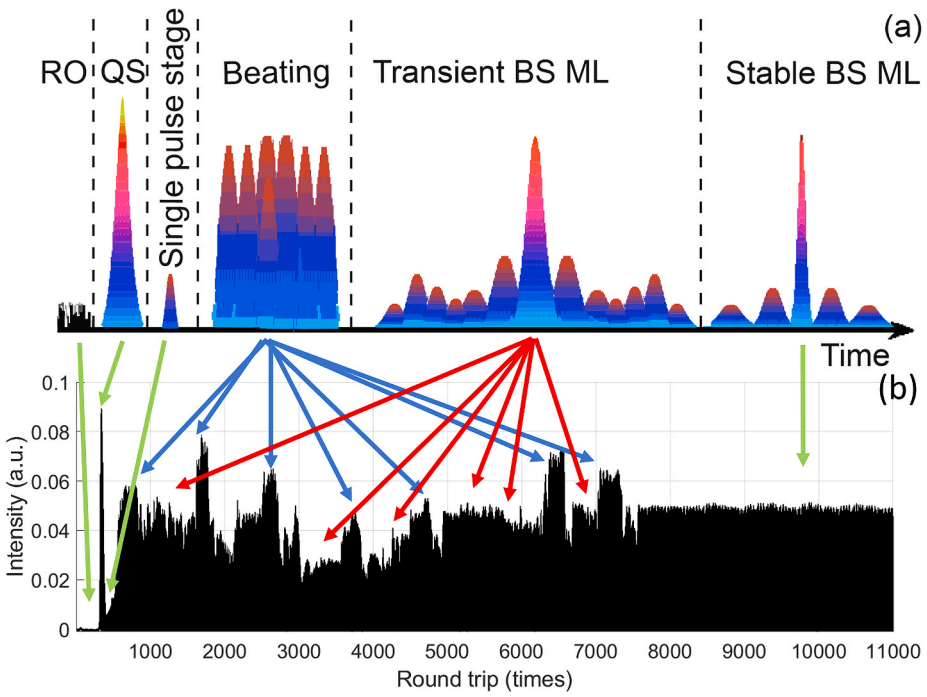

Fig. 2. Buildup process of solitons via Q-switching (QS). (a) Conceptual representation of the six soliton buildup stages. The QS pulse is twice higher of magnitude than the mode-locked (ML) soliton pulses. The first beating dynamics (BD) and Single pulse stages take less than 300 roundtrips time together. Multiple pulses coexist during the propagation, with one dominant pulse evolving into a soliton in the stable Bound state Modelocked (BS ML) stage. (b) Experimental results of the entire buildup process of laser stable BS ML. The time presented in fundamental soliton round trips. The QS stage is characterized by single high-intensity lasing spikes. Arbitrary units are denoted by a. u.

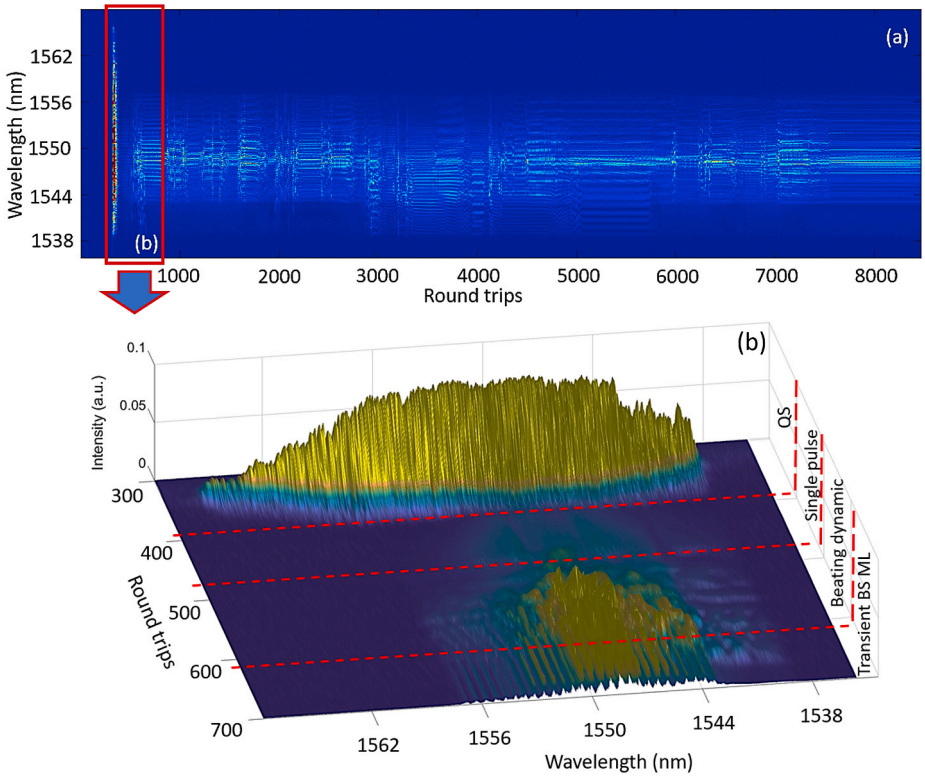

Fig. 3. Formation and evolution of a bound state with beating dynamics. (a) Experimental real-time interferograms. (b) A detailed 3D representation of the data captured between 300 and 700 round trips, which encompasses the stages of Q-switching (QS), transient single pulse, beating and transient bound state modelocked (BS ML) formation.

incrementally decrease the pump power. This approach is especially relevant in the context of mode-locked lasers where there is a marked hysteresis in relation to the pumping power, which is further intensified when dealing with multiple-pulse dynamics [39,40]. By progressively decreasing the pump power in both the NALM and UR, we managed to reduce the number of pulses within the bound state, and observed that the delay between the pulses increased correspondingly with the reduction in pump power. Ultimately, we decreased the total pump power from 650 mW to 160 mW, resulting in two bound pulses within the cavity with a temporal separation of approximately 100 ps (Fig. 5).

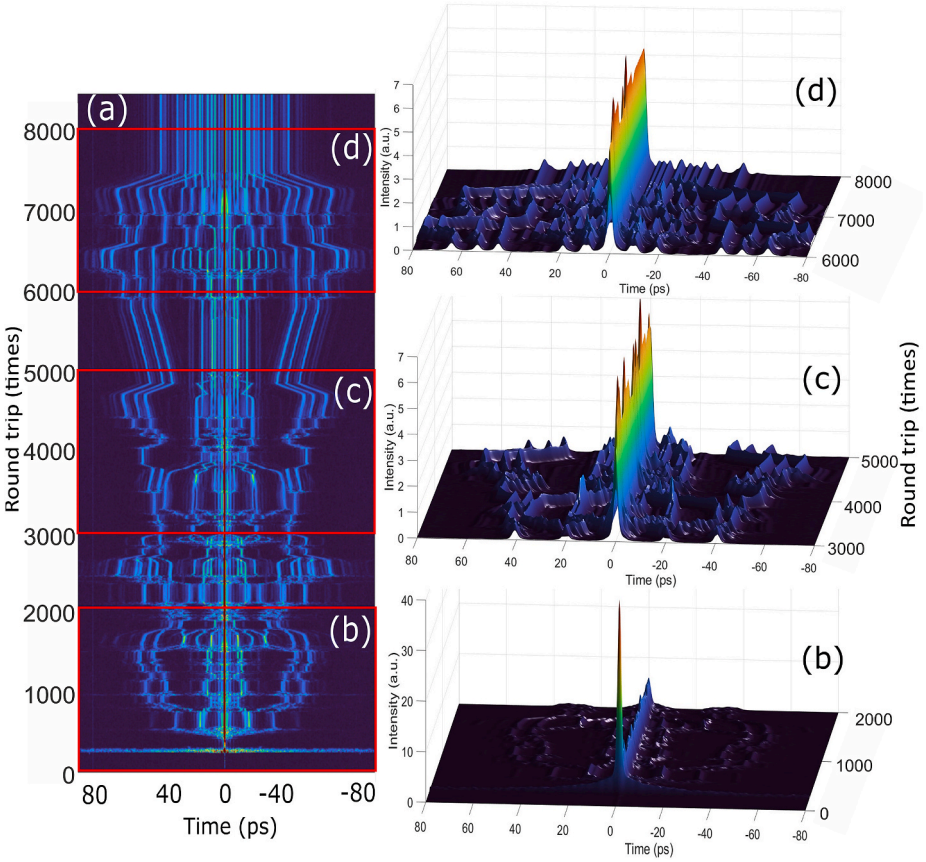

Fig. 4. The pulses dynamic during stable bound state formation. (a) The experimental real-time field autocorrelation traces calculated with the Fourier transform of each TS-DFT spectrum; A detailed 3D representation of the data captured between 1000 and 3000 (b), 4000 and 6000 (c), 7000 and 9000 round trips (d).

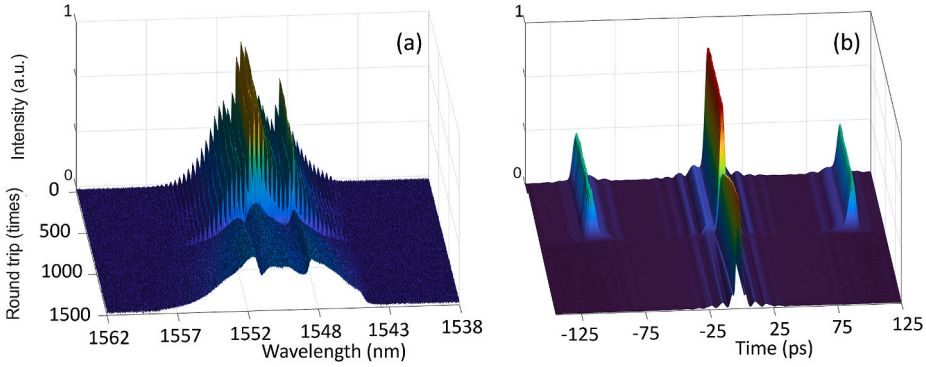

Fig. 5. Measured transition dynamic from the bound pulses to a single pulse in (a) spectral and (b) temporal domain by reducing the 980 nm pump power from 160 mW to 110 mW.

Further reduction of pump power eventually led to a single pulse mode-locked regime. This study marks the first, to our knowledge, to measure the transient dynamics from a dual pulse to a single pulse regime by decreasing power in an all-PM mode-locked laser. Fig. 5 provides an in-depth depiction of the transition phase from a two-pulse bound state to a single pulse mode-locked regime. The shot-by-shot experimental data, captured before and after this transition phase, portray both temporal and spectral information. As the round-trips progress (represented on the y-axis), the intensity profiles of the pulses (z-axis) evolve along with the intra-cavity time (x-axis). This transition phase took place for the time less than 10 round trips. In the time domain, the transient dynamic took less than 1 μs, thus establishing it as the fastest Mode-Locked (ML) dynamic switch from dual to single pulse mode that has been observed up until the present. The zero round trip depicted in Fig. 5 was captured just prior to the reduction of the pump power.

Our subsequent investigations primarily concentrated on the TS-DFT data associated with the single pulse stage. The spectral shape of the single pulse regime bore a resemblance to the transient single pulse stage observed during the build-up dynamics from QS to bound state ML (as seen in Fig. 3(b)). TS-DFT is among the few methods capable of measuring such rapid transient stages in the fiber laser cavity. Therefore, the subsequent step in our investigation was to compare the similarities between the single pulse regime in the build-up dynamic from QS to the unstable bound state, and the single pulse stage. According to Fig. 3 (b) we plot TS-DFT spectra and the field autocorrelation traces calculated

with the Fourier transform of this TS-DFT data. To accomplish this, we utilized data from the 450th roundtrip (the middle of the transient single pulse stage as illustrated in Fig. 3) of build-up from QS pulse dynamics and data from the 1500th roundtrip (shown in Fig. 5) TS-DFT. For a more comprehensive representation, we incorporated the autocorrelation trace, measured by a standard autocorrelator (Femtochrome FR-103XL), alongside the spectrum of the single pulse ML regime, analyzed by an Optical Spectrum Analyzer (Yokogawa AQ6370D).

Fig. 6 presents a comparison of autocorrelation traces and spectrum data recalculated from TS-DFT and measured by the optical spectrum analyzer and autocorrelator. The optical spectra and pulse duration of the single mode-locked pulse at the final stage, as measured by the TS-DFT (Fig. 6 b, f) and OSA/autocorrelator (Fig. 6 a, d), show similarity, with a slight discrepancy in pulse duration of 0.11 ps. The autocorrelator measured the pulse duration as 2.14 ps, while the pulse measured by the TS-DFT method was 2.33 ps.

The autocorrelation trace and spectra of the transient single pulse stage, measured by postprocessing data collected by the TS-DFT setup during build-up dynamics (Fig. 6 c, g), exhibit a spectral pattern closely resembling the spectra measured for the single mode-locked pulse at the final stage with a total pump power of 110 mW. The spectral bandwidth at Full Width at Half Maximum of the transient single pulse, measured using the TS-DFT method, is found to be 6 nm. This is narrower in comparison to the bandwidth of the stable single pulse, which is measured to be 7 nm by the Optical Spectrum Analyzer and by TS-DFT. This discrepancy is clearly due to the absence of accumulated Self-Phase Modulation within the laser cavity during the transient stage. Despite the low intensity of this pulse, its spectrum is discernible amidst the noise. The pulse duration of this single pulse is 0.78 ps, which approximates the Fourier limit of the generated spectra more closely than the pulse at 110 mW.

4. Conclusion

In this paper, we presented an analysis of the transient bound state soliton pattern in both time and frequency domains of an all-PM desperation-managed figure-eight mode-locked laser with NALM. Utilizing the Time-stretch Dispersive Fourier Transform method, we were able to measure rapid transient states within the laser cavity. We investigated different stages of build-up dynamics at different pump power, which includes a detailed analysis of the QS, transient single pulse formation, bound states, pulsation beating pattern and final transition to single pulse state. The results suggest that the mode-locked bound state regime does not originate directly from QS pulse or relaxation oscillations as it was previously published. Instead, it emerges from a single pulse stage subsequent to the QS pulse.

For the first time, we have experimentally depicted the transient single pulse stage of build-up dynamics, contrasting it with the fundamental mode-locked pulse of the system after reducing the pump power. Interestingly, our study observed a transition from a dual-pulse to a single pulse occurring in fewer than 10 roundtrips - a dynamic considerably faster than reported in previous studies.

This experimental research enriches the understanding of the complex dynamics in mode-locked lasers, providing valuable insights that will inform the design and optimization of future systems.

CRediT authorship contribution statement

D. Stoliarov: Investigation, Data curation, Formal analysis, Validation, Methodology, Software, Writing – original draft, Conceptualization. **I. Kudelin:** Methodology, Software, Writing – original draft. **A. Koviarov:** Investigation, Validation. **E. Rafailov:** Supervision, Conceptualization.

Declaration of competing interest

The authors declare that they have no known competing financial interests or personal relationships that could have appeared to influence the work reported in this paper.

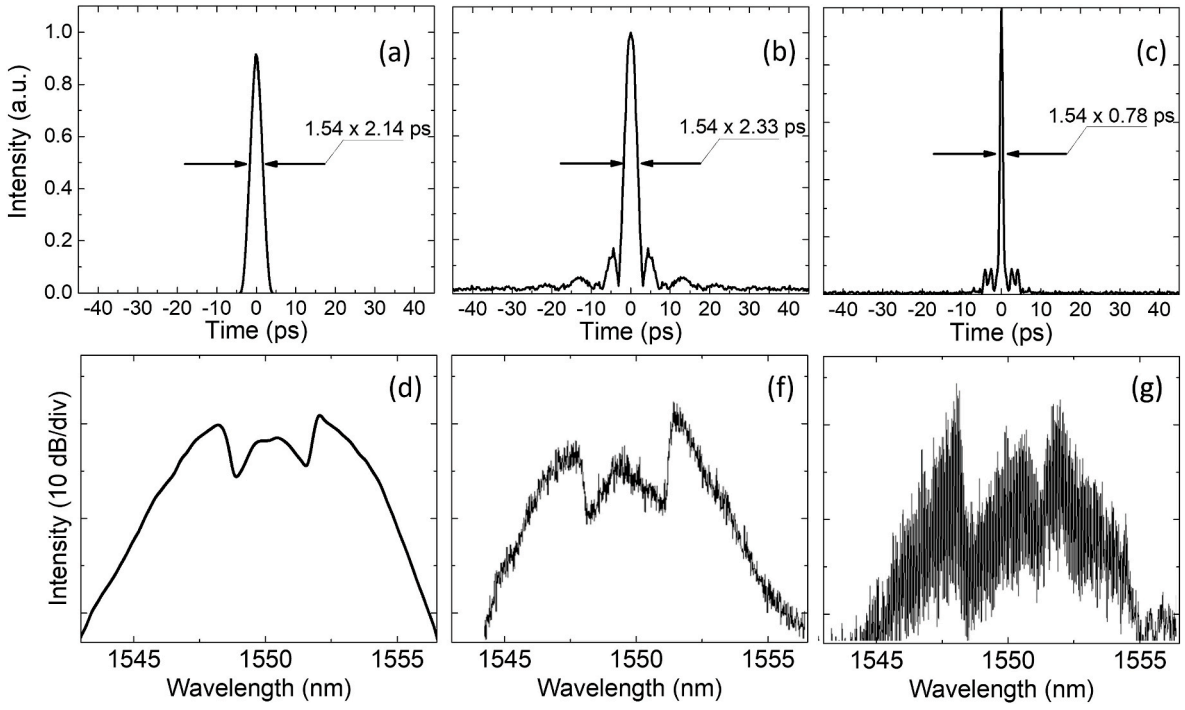

Fig. 6. Comparison of autocorrelation traces for the stable single pulse state at reduced pump power, measured by an autocorrelator (a) and TS-DFT (b), with a transient single pulse detected during the build-up of BS formation between Q-switching (QS) and Beating dynamics (c). Furthermore, a comparison of optical spectra for the stable single pulse state at reduced pump power, measured by an OSA (d) and TS-DFT (f), with a transient single pulse detected during the build-up of BS formation between QS and Beating dynamics (g).

Data availability

Data will be made available on request.

Acknowledgements

This research was supported by the EPSRC project EP/W002868/1 and the European Union's Horizon 2020 research and innovation programme under Grant Agreement 871277.

References

[1] R. Paschotta, Mode-locked Lasers: an Introduction, RP Photonics, 2021.
[2] U. Keller, Recent developments in compact ultrafast lasers, Nature 424 (2003) 831–838.
[3] O.G. Okhotnikov, Fiber Lasers, John Wiley & Sons, 2012.
[4] M.E. Fermann, I. Hartl, Ultrafast fibre lasers, Nat. Photonics 7 (2013) 868–874.
[5] D. Stoliarov, A. Koviarov, D. Korobko, D. Galiakhmetova, E. Rafailov, Fibre laser system with wavelength tuning in extended telecom range, Opt. Fiber Technol. 72 (2022), 102994.
[6] M. Wang, C. Chen, C. Huang, H. Chen, Passively q-switched er-doped fiber laser using a semiconductor saturable absorber mirror, Optik 125 (2014) 2154–2156.
[7] D. Stoliarov, P. Itrin, D. Korobko, V. Ribenek, L. Tabulina, A. Sysa, Y.P. Shaman, Saturable absorber based on the fiber coupler coated by cnts, Opt. Fiber Technol. 63 (2021), 102524.
[8] V. Matsas, T. Newson, D. Richardson, D.N. Payne, Self-starting, passively mode-locked fibre ring soliton laser exploiting non-linear polarisation rotation, Electron. Lett. 28 (1992) 1391–1393.
[9] Menlo Systems, Femtosecond Erbium Laser | Menlo Systems, 2023 [Online. (Accessed 2 June 2023).
[10] Femtosecond lasers - nkt photonics," Available at: https://www.nktphotonics.com/products/femtosecond-lasers/. Accessed: 2023-June-2.
[11] X. Liu, M. Pang, Revealing the buildup dynamics of harmonic mode-locking states in ultrafast lasers, Laser Photon. Rev. 13 (2019), 1800333.
[12] K. Goda, B. Jalali, Dispersive fourier transformation for fast continuous single-shot measurements, Nat. Photonics 7 (2013) 102–112.
[13] J. Chou, D.R. Solli, B. Jalali, Real-time spectroscopy with subgigahertz resolution using amplified dispersive fourier transformation, Appl. Phys. Lett. 92 (2008), 111102.
[14] A. Chong, J. Buckley, W. Renninger, F. Wise, All-normal-dispersion femtosecond fiber laser, Opt Express 14 (2006) 10095–10100.
[15] X. Wu, D. Tang, H. Zhang, L. Zhao, Dissipative soliton resonance in an all-normal-dispersion erbium-doped fiber laser, Opt Express 17 (2009) 5580–5584.
[16] D. Tang, L. Li, Y. Song, L. Zhao, H. Zhang, D. Shen, Evidence of dark solitons in all-normal-dispersion-fiber lasers, Phys. Rev. 88 (2013), 013849.
[17] N. Akhmediev, J.M. Soto-Crespo, G. Town, Pulsating solitons, chaotic solitons, period doubling, and pulse coexistence in mode-locked lasers: complex ginzburg-landau equation approach, Phys. Rev. E 63 (2001), 056602.
[18] J.M. Soto-Crespo, M. Grapinet, P. Grelu, N. Akhmediev, Bifurcations and multiple-period soliton pulsations in a passively mode-locked fiber laser, Phys. Rev. E 70 (2004), 066612.
[19] W. Chang, J.M. Soto-Crespo, P. Vouzas, N. Akhmediev, Extreme soliton pulsations in dissipative systems, Phys. Rev. E 92 (2015), 022926.
[20] R.J. Deissler, H.R. Brand, Periodic, quasiperiodic, and chaotic localized solutions of the quintic complex ginzburg-landau equation, Phys. review letters 72 (1994) 478.
[21] E.N. Tsoy, N. Akhmediev, Bifurcations from stationary to pulsating solitons in the cubic–quintic complex ginzburg–landau equation, Phys. Lett. 343 (2005) 417–422.
[22] H. Nakatsuka, D. Grischkowsky, A. Balant, Nonlinear picosecond-pulse propagation through optical fibers with positive group velocity dispersion, Phys. Rev. Lett. 47 (1981) 910.
[23] Z. Wang, Z. Wang, Y.-g. Liu, W. Zhao, H. Zhang, S. Wang, G. Yang, R. He, Q-switched-like soliton bunches and noise-like pulses generation in a partially mode-locked fiber laser, Opt Express 24 (2016) 14709–14716.
[24] G. Herink, F. Kurtz, B. Jalali, D.R. Solli, C. Ropers, Real-time spectral interferometry probes the internal dynamics of femtosecond soliton molecules, Science 356 (2017) 50–54.
[25] Z. Wang, K. Nithyanandan, A. Coillet, P. Tchofo-Dinda, P. Grelu, Optical soliton molecular complexes in a passively mode-locked fibre laser, Nat. communications 10 (2019) 830.
[26] P. Ryczkowski, M. Närhi, C. Billet, J.-M. Merolla, G. Genty, J.M. Dudley, Real-time full-field characterization of transient dissipative soliton dynamics in a mode-locked laser, Nat. Photonics 12 (2018) 221–227.
[27] D. Deng, H. Zhang, J. Zu, J. Chen, Buildup dynamics of a pulsating dissipative soliton in an all-normal-dispersion pm yb-doped fiber laser with a nalm, Opt. Lett. 46 (2021) 1612–1615.
[28] G. Herink, B. Jalali, C. Ropers, D.R. Solli, Resolving the build-up of femtosecond mode-locking with single-shot spectroscopy at 90 mhz frame rate, Nat. Photonics 10 (2016) 321–326.
[29] J. Peng, M. Sorokina, S. Sugavanam, N. Tarasov, D.V. Churkin, S.K. Turitsyn, H. Zeng, Real-time observation of dissipative soliton formation in nonlinear polarization rotation mode-locked fibre lasers, Commun. Phys. 1 (2018) 20.
[30] I. Kudelin, S. Sugavanam, M. Chernysheva, Build-up dynamics in bidirectional soliton fiber lasers, Photon. Res. 8 (2020) 776–780.
[31] I. Kudelin, S. Sugavanam, M. Chernysheva, Pulse-onset dynamics in a bidirectional mode-locked fibre laser via instabilities, Commun. Phys. 3 (2020) 202.
[32] Q. Hao, F. Chen, K. Yang, X. Zhu, Q. Zhang, H. Zeng, Self-started mode-locking with dispersion-imbalanced nonlinear amplifier loop, IEEE Photon. Technol. Lett. 28 (2015) 87–90.
[33] D. Kirsch, S. Chen, R. Sidharthan, Y. Chen, S. Yoo, M. Chernysheva, Short-wave ir ultrafast fiber laser systems: current challenges and prospective applications, J. Appl. Phys. 128 (2020), 180906.
[34] T. Ennejah, F. Bahloul, M. Salhi, R. Attia, Optimization of passive and hybrid mode-locked figure eight laser, J. Opt. Commun. 34 (2013) 179–185.
[35] J. Theimer, J. Haus, Figure-eight fibre laser stable operating regimes, J. modern Opt. 44 (1997) 919–928.
[36] S. Boscolo, C. Finot, I. Gukov, S.K. Turitsyn, Performance analysis of dual-pump nonlinear amplifying loop mirror mode-locked all-fibre laser, Laser Phys. Lett. 16 (2019), 065105.
[37] X. Liu, X. Yao, Y. Cui, Real-time observation of the buildup of soliton molecules, Phys. review letters 121 (2018), 023905.
[38] F. Kurtz, C. Ropers, G. Herink, Resonant excitation and all-optical switching of femtosecond soliton molecules, Nat. Photonics 14 (2020) 9–13.
[39] C.L. Campos, L.H. Acioli, M.H. de Miranda, Hysteretic behavior for transmission curve and soliton temporal separation in multi-pulsing regime for mode-locked fiber lasers, Laser Phys. 31 (2021), 085103.
[40] A. Zavyalov, R. Iliew, O. Eogrov, F. Lederer, Hysteresis of dissipative soliton molecules in mode-locked fiber lasers, Opt. letters 34 (2009) 3827–3829.